μ-PPTs diagnostics: a high accuracy impulsive thrust balance

IEPC-2013-165

Presented at the 33rd International Electric Propulsion Conference,
The George Washington University • Washington, D.C. • USA
October 6 – 10, 2013

S. Ciaralli[1]
University of Southampton, Southampton, UK, SO17 1BJ

M. Coletti [2]
Mars Space Ltd, Southampton, UK, SO14 5FE

and

S. B. Gabriel[3]
University of Southampton, Southampton, UK, SO17 1BJ

This paper describes the design and testing of a direct torsional impulsive thrust balance. The design philosophy allows the balance to measure impulse bits (*Ibit*) in the range of 20 – 120 μNs typical of Pulsed Plasma Thrusters (PPTs) for pico and nano-satellite. The uncertainty in the *Ibit* measurement is quantified to be about 8.8 %, smaller than the typical values of this kind of balances (between 12 and 15%). This has been possible due to an in-depth analysis of all the possible sources of disturbance, which allows the choice of the most suitable measurement and estimation methods to minimize the errors. The balance has successfully been used for testing two PPTs with different propellant feeding system, nominal energy, mass and delivered impulse bits.

Nomenclature

E	=	initial energy
FT	=	Fourier Transform
f_{nat}	=	natural oscillation frequency
H	=	balance transfer function
Ibit	=	impulse bit
J	=	total momentum of inertia
J_{arm}	=	balance arm momentum of inertia
J_{cw}	=	counterweight momentum of inertia
J_{th}	=	thruster momentum of inertia
J_{weight}	=	testing weight momentum of inertia
k	=	torsional elastic constant
N	=	noise
PPT	=	Pulsed Plasma Thruster

[1] PhD student, Physical Sciences and Engineering, sc2d11@soton.ac.uk
[2] Director, Michele.coletti@mars-space.co.uk
[3] Professor, Physical Sciences and Engineering, sgb2@soton.ac.uk

RMS = Root Mean Square
r_{sens} = distance between sensor head and rotational axis
r_{th} = distance between PPT and rotational axis
T = thrust
t = time
V_0 = initial capacitor bank voltage
x = fitted displacement signal
x_{sens} = acquired displacement signal
Ψ = output sensor signal
α = optical sensor sensitivity
λ = damping coefficient
θ = angular displacement
ω = angular velocity
ω_0 = natural angular velocity

I. Introduction

In recent years the miniaturization of spacecraft subsystems has been boosted by the development of nano and pico satellites, i.e. Cubesats that allow for cheap and quick access to space. The orbit lifetime of Cubesats is normally determined by the natural drag-induced de-orbiting as they are normally launched into sun-synchronous or low earth orbits at an altitude between 250 and 650 km. A propulsion system that matches the miniaturized dimensions and the low cost of such kind of satellites may be used to achieve orbital control. Electric propulsion systems are usually lighter and provide better performance than the conventional chemical-based system, e.g. cold gas thruster[1]. In electric propulsion thruster the propellant is accelerated either by electrothermal, electrostatic or electromagnetic means. Among the miniaturized electric thrusters, solid propellant Pulse Plasma Thrusters (PPTs) represent a good choice for nano and pico satellites propulsion systems[2]. This kind of PPT is characterized by a high scalability in terms of geometry, power consumption and performances. Moreover they do not require tanks and valves. The impulse bit (*Ibit*) produced by these μ-PPTs is in the range of 20-150 μNs, with an input power lower than 10 W[3]. This paper describes an impulsive thrust balance that has been designed to measure the *Ibit* of μ-PPTs. The balance has been tested using two different PPTs that the University of Southampton, in collaboration with Mars Space Ltd and Clyde Space Ltd have designed and developed. The first thruster is a breech-fed PPT for nano-satellite applications, designed to provide about 90 μNs with an input power of 5 W [4]. The second thruster is a side-fed PPT for Cubesat orbital control which, at the time of writing, is undergoing flight qualification[5].This has been designed to provide about 40 μNs with an input power of 2 W [6].

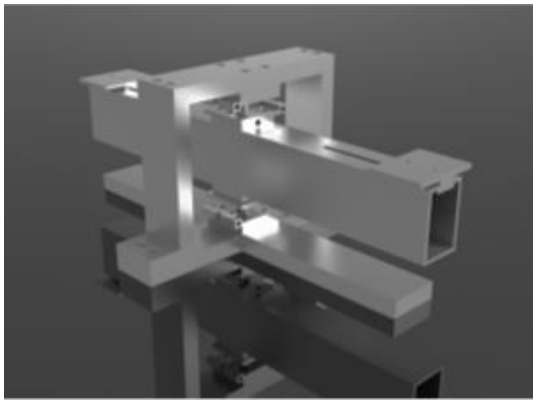

Figure 1. Mechanical design of the balance

Sub-millinewton impulsive thrust measurements have already been performed in the past both indirectly by installing the measurement system target in the path of the ejected propellant[7] and directly by mounting the thruster to the measurement system[8]. Direct measurement techniques are considered more accurate and most suitable for PPT applications. Their main disadvantage is that propellant feed lines and electrical connections can generate thermal and mechanical stresses and drifts of the same order of magnitude of the thrust to measure. However solid propellant PPTs do not have propellant feed lines and the electrical connections will most likely not produce any thermal stress or drift since the PPTs firing frequency is in the range of 0.1 – 10 Hz and the power input lower than 10W [9].

Both direct and indirect measurements are typically performed by hanging[10] or torsional pendulums[11]. Their main advantage lies in the simplicity of construction and low cost.

Hanging balances are characterized by high stability and low gain. To obtain high sensitivity a long pendulum arm is required and this is impractical for small test facilities[7].

Unlike hanging pendulum configuration, in a torsional pendulum the restoring force is independent of the thruster mass, as the rotational axis is parallel to the gravity vector. High sensitivity can be obtained by increasing the arm length (leading to the same issue found for hanging pendulum) or by selecting suitable low stiffness supporting flexures.

Regarding the measurement of the pendulum displacement different techniques have previously been used and they include strain gauges[12], capacitive[13], linear transducer[14] and interferometric techniques[15]. As the system displacement is inherently small (of the order of 10 μm) due to typical *Ibit* values, non-contact techniques offer the least potential of interference with the measurement.

In the present configuration, shown in figure 1, a direct measurement system has been selected for its simplicity and low cost. The system consists of a non-contact laser optical sensor used for measuring the angular displacement θ of a torsional pendulum arm. As μ-PPTs provide thrust that typically lasts few microseconds, the balance is designed to work as a free oscillations compound pendulum. To dissipate oscillatory motions and thus to reduce the time between two consecutive measurements, it would be possible to use a magnetic damping system. Even if passive eddy-current systems have previously been used[7,14], they have not been included in the present system. The balance itself can dissipate the oscillatory motions in less than three minutes, as shown in figure 2. This value can be considered acceptable because of the inherently simplicity of the measurement system.

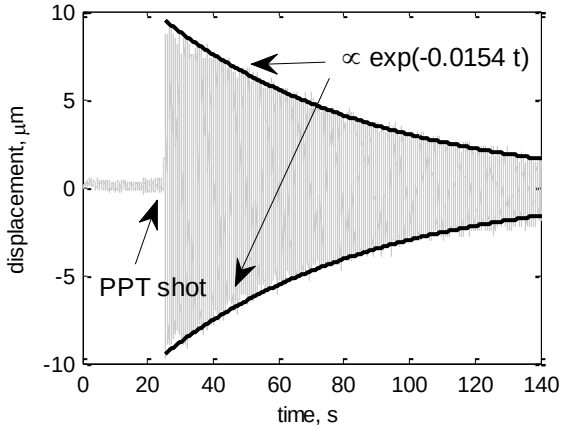

Figure 2. Natural balance damping after a PPT shot

Finally even if the estimation of the error in *Ibit* measurement is essential for the development of a thrust balance, few authors[10-11] have presented all the details and the assumptions used for the error quantification. In this paper, the analysis of the sources of disturbance, the most convenient methods of measurements and the details of the error estimation are reported for the first time for this type of balance.

II. The experimental apparatus

A. The vacuum chamber

The vacuum facility used to replicate the space environment consists of a 0.6 m diameter by 1.2 m long chamber. Vacuum pumping is achieved with a water-cooled turbo molecular pump (Pfeiffer Balzers TPH 2200) backed by a rotary vane pump (Edwards E2M80). Vacuum pressure is monitored with a Balzers TPG251 pressure gauge package. During the tests, the chamber pressure has always been maintained below 1.0×10^{-5} mbar.

B. The thrust balance

The balance consists of a horizontal pendulum arrangement with the thruster mounted on one end of the arm and a counterbalance on the other. The balance is symmetrical with respect to the arm rotation axis with the counterweight and the thruster positioned at the same distance from the central rotating pivot, as shown in figure 3.

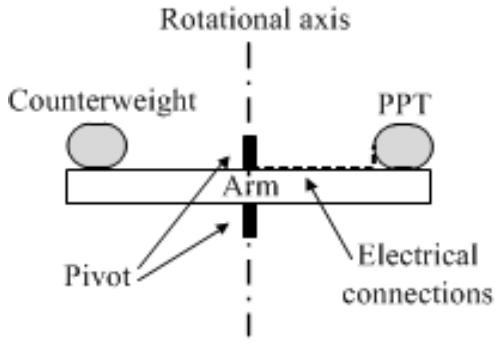

Figure 1. Thrust stand schematic (not in scale)

This will eliminate the error due to gravity effects. All the parts are made out of 6068-T6 aluminium alloy except for the centre pillar that is made out of 302 grade stainless steel. The pillar is mounted through the centre of rotation and in between the two pivots going through the whole of the arm. The balance arm has a rectangular section (50 x 75 mm) and an overall length of 550 mm.

Two stainless steel flexural pivots from Riverhawk Co. (5016-600 model) have been chosen for this balance. They are used to constrain the arm so it only has one degree of freedom. They have very low friction and virtually no hysteresis at the rotations expected during normal operation[16]. This makes them more desirable than conventional ball bearings and magnetic bearings, as flexural pivots are elastic elements easily designed, they do not require a control system for stability, they are vacuum compatible and their low cost is a significant advantage. Their nominal spring constant value is 0.7334 Nm/rad.

Three cables, fixed on the top surface of the balance arm, are used to feed the PPT providing the voltage to apply to its capacitor bank and to trigger the main discharge[2]. These cables affect the value of the balance torsional elastic constant (further details in section 3.2.2) whereas their influence in term of total momentum of inertia about the rotational axis is negligible being the ratio between the balance arm and the cables momenta of inertia < 0.1%.

C. The displacement sensor

The displacement of the balance arm around the axis of rotation is measured with a fibre optic linear displacement sensor. These kinds of sensors have previously been used for measuring thrust balance arm displacement[8, 17].

For this balance the DB63 fibre-optic sensors from Philtec Inc. in the US have been selected[18]. This sensor sends out a LED signal through a fibre-optic cable to the cable head pointed at the target. Then a second cable running parallel to the input one is used to measure the amount of the signal that is reflected. From this, the distance between the sensor head and the target can be calculated to high accuracies. Once calibrated adjusting the gain on the sensor controller, the sensor shows an optical peak at about 150 μm, corresponding to the distance between the target and the sensor head when the maximum reflectance is measured. The sensor can be operated on either side of this peak, near-side for closer operation (from 0 μm to 150 μm) or far-side for larger distances (from 150 μm up to 3 mm). As the expected balance displacement has the order of magnitude of few micrometres, near-side configuration has been chosen to perform the measurement. This configuration yields the highest possible sensor resolution of about 50 nm. The sensor output is between 0 and 5 V and it is acquired and displayed by a Tektronix DPO3014 oscilloscope.

The sensor head is mounted pointing at the arm and placed at about 40 μm from the balance arm in order for it to work in the center of the calibration curve linear region (shown in figure 4). To adjust the sensor head position a sliding micrometer screw from Standa Ltd (9S75M micrometer screw with a resolution of 2.5 μm mounted into a 7T67V-25 linear stage) has been chosen.

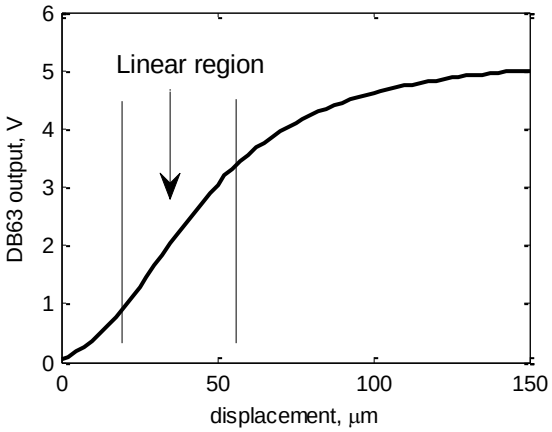

Figure 2. Optical displacement sensor characteristic. Near-side configuration.

III. Performances

D. Impulse bit measurement

Being a torsional pendulum, the balance can only detect the force component perpendicular to the balance arm and to the rotational axis. If the thruster is not aligned, the parallel thrust component will not be detected. The PPT is mounted on the balance with the misalignment angle < 1°. In this condition the parallel thrust component proportional to the sine of this angle is negligible. Thus assuming that the thrust is perpendicular to the balance arm, the dynamics of a torsional balance are described by the harmonic oscillator equation

$$J\ddot{\theta}(t) + \lambda\dot{\theta}(t) + k\theta(t) = r_{th}T(t) \tag{1}$$

where θ is the angular displacement, J is the total momentum of inertia about the rotational axis, λ is the damping coefficient, k is the total torsional elastic constant, and $T(t)$ is the applied thrust at the distance r_{th} from the rotational axis (figure 5). If t_{shot} is the PPT discharge time the thrust can be modeled[11] as

$$T(t) = \begin{cases} T & 0 \le t \le t_{shot} \\ 0 & t > t_{shot} \end{cases} \tag{2}$$

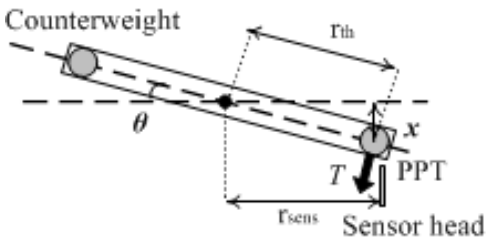

Figure 3. Balance arm schematic (not in scale)

Considering the general solution of (1) for $0 \le t \le t_{shot}$ and assuming that $t << t_{nat}$, where t_{nat} is the balance natural oscillation period, it can be demonstrated[19] that at $t = t_{shot}$

$$\theta(t_{shot}) \approx 0, \quad \dot{\theta}(t_{shot}) \approx \frac{r_{th} T}{J} t_{shot} = \frac{r_{th} Ibit}{J} \tag{3}$$

Using (3) as initial values of the homogeneous differential equation (1) for $t > t_{shot}$ leads to

$$\theta(t) = \frac{r_{th} Ibit}{J\omega_0} \exp\left(-\frac{\lambda}{2J} t\right) \sin(\omega_0 t) \tag{4}$$

where ω_0 is by definition

$$\omega_0 = \sqrt{\frac{k}{J}} = \frac{2\pi}{t_{nat}} = 2\pi\ f_{nat} \tag{5}$$

From (4) the maximum amplitude θ_{max} is defined as

$$\theta_{\max} = \frac{r_{th} Ibit}{J\omega_0} \tag{6}$$

For small angular displacements the displacement Δx_{max} measured by the optical sensor is given by

$$\Delta x_{\max} = r_{sens} \sin(\theta_{\max}) \approx r_{sens} \theta_{\max} \tag{7}$$

where r_{sens} is the distance of the sensor head from the rotational axis.

Combining (5), (6) and (7) it can be obtained the following expression for the *Ibit* evaluation

$$Ibit = \frac{2\pi\ f_{nat}\ J\ \Delta x_{\max}}{r_{sens} r_{th}} \tag{8}$$

E. Balance characterization

According to (8), to evaluate the *Ibit* provided by the thruster five parameters have to be measured or calculated, i.e. the natural frequency f_{nat}, the total momentum of inertia J, the maximum displacement Δx_{max} measured by the optical sensor and the distances r_{th} and r_{sens} from the rotational axis.

1. Natural frequency evaluation

The natural oscillation frequency f_{nat} depends on balance arm length and cross section and on the mass and position of the thruster that is under test and the counterweight. It is also influenced by the electrical wires fixed on the top of the balance that feed the thruster. However f_{nat} can be easily calculated as the peak of the Fourier transform (FT) of the acquired displacement signal, as shown in figure 6.

This method of measurement takes into account the effects of all the possible sources of influence. It requires the processing of the signal acquired once the balance is set in the final arrangement with the PPT and the counterweight located on the arm tips and the electrical wires connected to the thruster.

The error on f_{nat} measurement is proportional to the ratio between the signal sampling frequency and the number of acquired samples[20]. Thus the signal is acquired using an oscilloscope with a sampling frequency of at least 25 kHz for a time of at least 2 minutes. The uncertainty in f_{nat} measurement has an order of magnitude of 1 mHz. As f_{nat} has an order of magnitude of 1 Hz, the error is < 1 % and can be considered negligible.

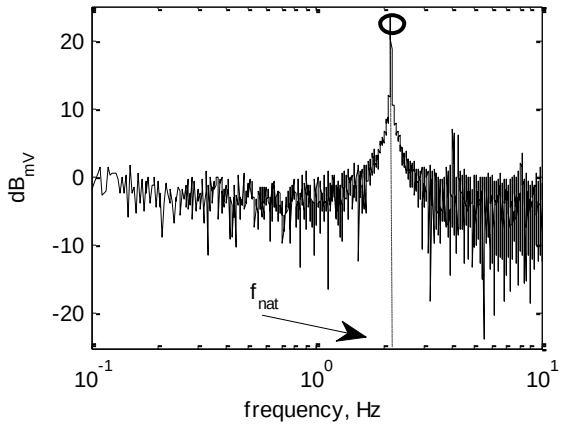

Figure 4. Example of FT used to evaluate the natural oscillation frequency. In the picture f_{nat} = 2.145 ± 0.003 Hz.

2. *Moment of inertia evaluation*

The total momentum of inertia J can be expressed as

$$J = J_{arm} + J_{th} + J_{cw} \tag{9}$$

where J_{arm}, J_{th} and J_{cw} are respectively the momentum of inertia of the balance arm, the thruster under test and of the counterweight. J_{arm} has been evaluated by adding different cylindrical weights on the balance arm and calculating the relative natural oscillation frequency. If two weights having the same shape and size are located symmetrically to the rotational axis, (9) can be written

$$J = J_{arm} + 2J_{weight} \tag{10}$$

where the momentum of inertia of the tested weight J_{weight} is known. Combining (5) and (10) it can be obtained

$$2\omega^2 J_{weight} = -J_{arm}\omega^2 + k \tag{11}$$

As ω is calculated with the FT of the acquired signal, (11) is in the form of a straight line equation, where the absolute value of the slope is J_{arm} and the intercept is the torsional elastic constant. The weights used for this test are made of steel and have a cylindrical shape. Their mass has been measured with a high resolution mass balance (Metter Toledo, model XP205, with a resolution of 10 µg), whereas their diameter and height have been measured using a caliper (resolution 0.25 mm). The error in J_{weight} is hence < 1%.

Repeating the measurements changing the pair of weights and acquiring the relative ω, it has been possible to fit the test results hence evaluating the balance arm momentum of inertia and torsional elastic constant (figure 7).

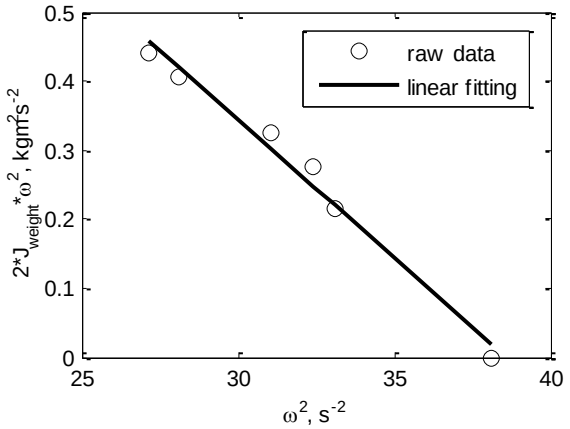

Figure 5. Linear fitting results to evaluate J_{arm} (slope) and k (y-axis intercept). Error bars are not shown because they would not be visible.

The values of J_{arm} and k and their relative uncertainties[21] δJ_{arm} and δk are summarized in table 1. Note that these values take into account the mechanical influence of the electric wires fixed on the top of balance.

Table 1. Balance momentum of inertia and torsional elastic constant

	Value (from linear fitting)
J_{arm} (kgm^2)	40.2E-3 ± 2.7E-3
k (Nmrad^{-1})	1.550 ± 0.086

J_{th} and J_{cw} that appear in (9) and their relative uncertainties are known once the thruster to test is set on the balance arm. J_{th} is a geometrical property of the thruster and the counterweight is chosen and placed on the balance arm in order to have $J_{cw} \approx J_{th}$.

3. Arm displacement evaluation

The evaluation of the maximum arm displacement Δx_{max} is obtained by fitting the ideal thrust stand response $x(t)$ to the real displacement signal $x_{sens}(t)$ acquired with the optical sensor using the standard least square method. This strategy has previously been used by other authors[11,22,23]. Combining (4) and (7) it can be obtained

$$x(t) = \Delta x_{\max} \exp\left(-\frac{\lambda}{2J}t\right)\sin(\omega t) \tag{12}$$

As shown in figure 8 the acquired data xsens(t) always include noise mainly due to background vibrations, i.e. turbo pumps,. However the turbo molecular pump rotates at about 36000 rpm, hence inducing vibrations that have a frequency spectrum peak at about 600 Hz. Considering the data in table 1 and typical µ-PPTs mass[3] (< 400 g), the thrust stand has a natural oscillation frequency less than 3 Hz. In the present configuration, turbopump induced noise doesn't significantly affect xsens(t) (see Appendix B) and the data fitting can always be performed with a goodness estimated in terms of R-square coefficient[21], greater than 0.98. Figure 8 shows an example of the fitting of xsens(t) using x(t) in (12) fitting.

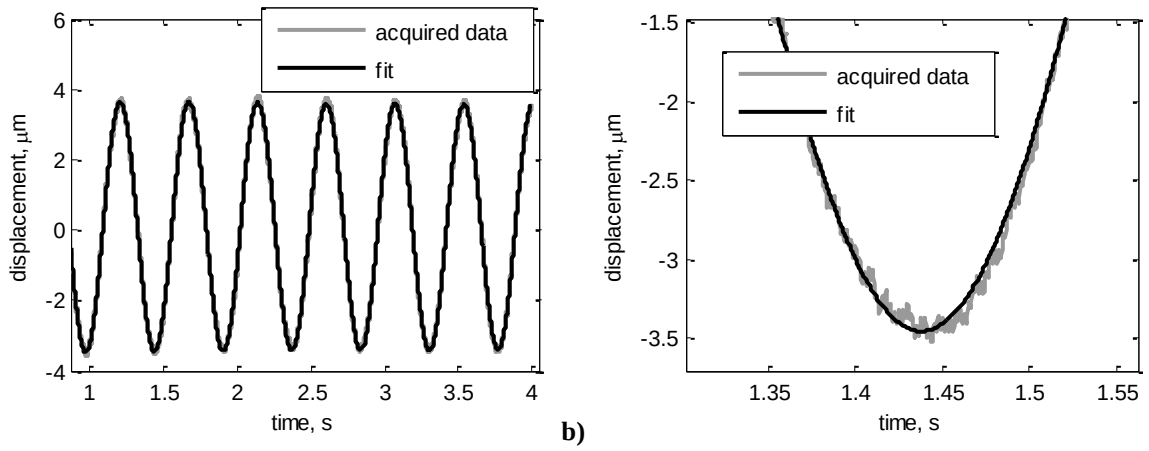

Figure 6. Example of acquired displacement signal (grey curve) and its best fitting (black curve): a) complete acquire signals, b) details of fitting. R-square = 0.9986

The raw optical sensor output signal $\Psi(t)$ is a 0 - 5 V signal. The gap between the sensor head and the balance arm is selected by the micrometer screw to allow the sensor to work in the linear region of its characteristic curve, as shown in figure 4. If α is the slope of the characteristic in the linear region, the following equation can be obtained:

$$x_{sens}(t) = \alpha \Psi(t) \tag{13}$$

The optical sensor is calibrated before starting the *Ibit* measurement by acquiring the output signal $\Psi(t)$ at different values of the gap between the sensor head and the balance arm. The gap is modified using a sliding micrometer screw. From the data so obtained the linear region of the sensor characteristic is selected and fitted (figure 9) to determine the value of α and its uncertainty $\delta\alpha$ using the common equations of the statistics fitting[21].

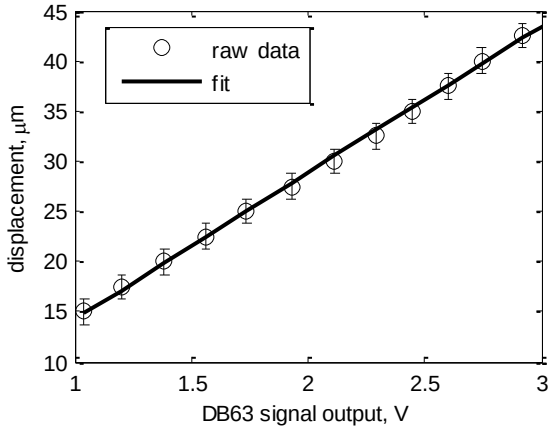

Figure 7. Example of optical sensor linear region characteristic fitting.

Taking into account the sliding micrometer screw resolution (± 1.25 μm) it has been found that $\delta\alpha/\alpha$ is typically < 4%.

The error in voltage signal $\Psi(t)$ acquisition is related to the resolution of the oscilloscope used for the measurement (± 5 mV[24]). As the typical $\Psi(t)$ values are in the range between 1 and 3 V in the linear region of the sensor characteristic, the relative error $\delta\Psi/\Psi$ is always ≤ 0.5 %. In the present configuration it has been chosen $\delta\Psi/\Psi$ = 0.5 % for a more conservative error evaluation.

4. Sensor head and thruster distances from rotational axis

The optical sensor head is placed close to the edge of the balance arm to maximize the acquired arm displacement according to (7). The distance r_{th} is known once the thruster is set on the balance arm. The values of these distances are measured with a caliper. In the present arrangement r_{sens} = 270 ± 1 mm.

F. Error budget

The relative uncertainty in *Ibit* measurement is calculated as

$$\frac{\delta Ibit}{Ibit} = (1+\beta)\cdot\sqrt{\left(\frac{\delta r_{rth}}{r_{rth}}\right)^2+\left(\frac{\delta J}{J}\right)^2+\left(\frac{\delta f_{nat}}{f_{nat}}\right)^2+\left(\frac{\delta r_{rsens}}{r_{rsens}}\right)^2+\left(\frac{\delta \Delta x_{\max}}{\Delta x_{\max}}\right)^2} \tag{14}$$

It is derived by (8) as all the terms that appear in it can be independently measured and their errors are not correlated[25].

The first four terms of (14) are known once the PPT to test has been chosen and set on the balance arm with its suitable counterweight. According to (13) the relative uncertainty in Δx_{max} can be express as

$$\frac{\delta \Delta x_{\max}}{\Delta x_{\max}} = \sqrt{\left(\frac{\delta \alpha}{\alpha}\right)^2+\left(\frac{\delta \Psi}{\Psi}\right)^2} \tag{15}$$

In (14) the term β has been added to take into account all the unpredictable sources of disturbance, e.g. misalignment angle and thrust vector divergence[26], thus a more conservative *Ibit* error evaluation is achieved. Considering all the assumptions and the reliability of the thrust stand, it has been arbitrarily chosen β = 10% for a worst case estimate of the error. Table 2 summarizes the value of all the terms in (14).

Table 2. Error budget summary.

	Value (%)
$\delta r_{th}/r_{th}$	0.3
$\delta r_{sens}/r_{sens}$	< 0.5 [a]
$\delta f_{nat}/f_{nat}$	< 0.5 [a]
$\delta J/J$	< 7 [a]
$\delta\alpha/\alpha$	3.8
$\delta\Psi/\Psi$	0.5

[a] The exact value depends on the actual PPT under test

In the present configuration, the uncertainty in *Ibit* measurement is 8.8 %. This value is smaller than the error values (about 15%) that characterize other impulsive torsional pendulums for μ-PPTs applications[19, 27].

IV. Impulse bit measurement

The present impulsive thrust balance has been used to measure the *Ibit* of two different μ-PPTs.

The first PPT is a side-fed PTFE propellant thruster for Cubesats application. It has a 1.6 μF capacitor bank, a nominal initial energy E = 2 J and an overall mass of about 120 g. At the moment, this PPT is under the final qualification test. The previous breadboard model has been fully characterized in 2011[6] and its *Ibit* was measured with a thrust balance at the University of Stuttgart[27]. Figure 10 shows the comparison between these results and the qualification model performance measured with the present thrust stand. The value of *Ibit* evaluated with the present thrust balance is the average of about 100 measurements uniformly performed during the first half of the PPT lifetime test (≈ 4E5 shots) [5]. In the breadboard model, the *Ibit* to *E* ratio is about 17.0 ± 2.1 μNs/J, whereas in the new model *Ibit/E* is 19.3 ± 1.5 μNs/J. The value measured using the present balance matches the previous test

results within the relative error bars and it is in the range of the typical side-fed *Ibit/E* values, whose upper limit is estimated[2] in about 23μNs/J.
The second PPT that has been tested is a breech-fed PTFE propellant thruster for nano-satellites application. This breadboard model[4] has a 4 μF capacitor bank, a nominal initial energy E = 5 J and an overall mass of about 300 g. Figure 11 shows the results of the measurements performed at different initial E and the results lead to an *Ibit/E* = 15.9 ± 1.3 μNs/J. This is in accordance to the typical[2, 28] breech-fed *Ibit/E* value of 16 μNs/J.
In both the examples the error in E measurements is negligible (less than 1 %).

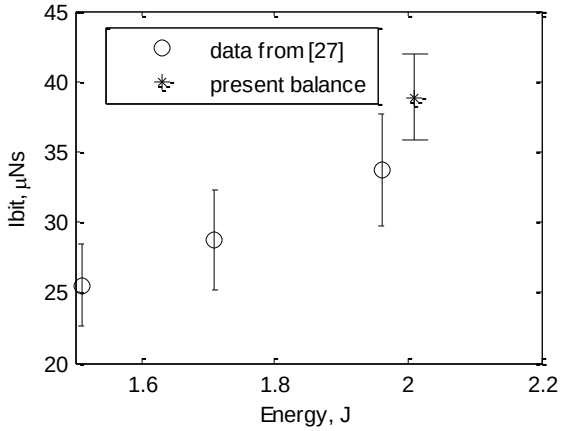

Figure 8. Side-fed PPT performances comparison.

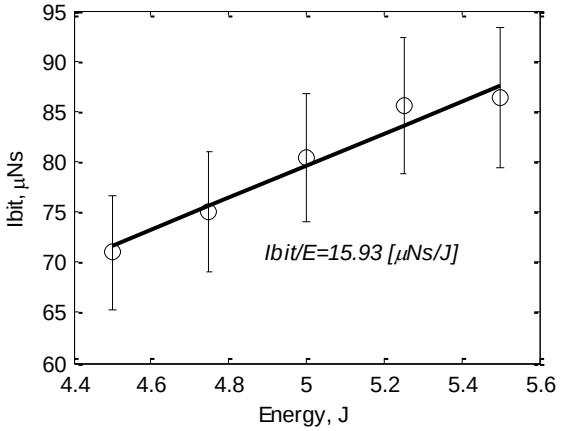

Figure 9. Breech-fed PPT Ibit measurements

V. Conclusions

The design of a low cost torsional pendulum impulsive thrust balance has been presented. This device is essential in the development of the μ-PPTs that the University of Southampton is carrying out in collaboration with Mars Space Ltd and Clyde Space Ltd.
The uncertainty on the *Ibit* measurement is 8.8%. Although all the known possible sources of disturbance have been taken into account and the reliability of the final arrangement, the error in the *Ibit* measurement has been arbitrarily increased by a factor $\beta = 10$ % to include the unpredictable sources of error. The error that characterizes the present balance is smaller than the typical error budgets of other balances for μ-PPTs applications[19, 27]. However, even the unrealistic choice of a factor $\beta = 100$ % would still only lead to a total uncertainty of 16 %. By taking into account all of known sources of uncertainty, it has been possible to significantly decrease the uncertainty in the measurement of *Ibit* over previous measurements even allowing for unknown uncertainties. This could be of importance not only for ground verification of thruster performance but for design to meet a given specification (for example, when trying to meet very precise pointing requirements) or comparison with flight data.

The thrust stand has been used to test two μ-PPTs with different propellant feeding system, nominal energy and mass have been tested and the measurement results presented. The side-fed PPT for Cubesat application is characterized by an *Ibit/E* = 19.3 ± 1.4 μNs/J, whereas in the breech-fed PPT for nano-satellite applications it has been found *Ibit/E* = 15.9 ± 1.3 μNs/J. These results match the typical values reported in the relevant literature.

Appendix. Noise analysis

Acquired data are always affected by the mechanical noise induced on the balance by background vibrations, i.e. turbo pumps. In this case, considering (5), the dynamics of a torsional balance can be express in term of arm displacement *x(t)* by the following equation:

$$\ddot{x}(t) + 2\zeta\,\dot{x}(t) + \omega_0^2 x(t) = \frac{r_{sens}}{J} N(t) \tag{B.1}$$

where *N(t)* is the torque induced by the vibrations and ζ is by definition

$$\zeta = \frac{\lambda}{2J} \tag{B.2}$$

Performing the Laplace transform to (B.1) and taking into account the initial conditions of the problem reported in (3), the following equation can be evaluated:

$$X(s) = H(s)N(s) + H(s)r_{th}Ibit = X_N(s) + X_{sol}(s) \tag{B.3}$$

where the balance transfer function *H(s)*, shown in figure B1, is given by:

$$H(s) = \frac{r_{sens}/J}{s^2 + 2\zeta s + \omega_0^2} \tag{B.4}$$

For (B.3) the solution *X(s)* consists of two terms: $X_N(s)$ which is due to the noise and $X_{sol}(s)$ which is the ideal solution. Note that the inverse Laplace transform of the latter term is equivalent to (12).
Since (B.1) and the Laplace transform operator are linear, the effect of the noise can be analysed considering only the term $X_N(s)$.

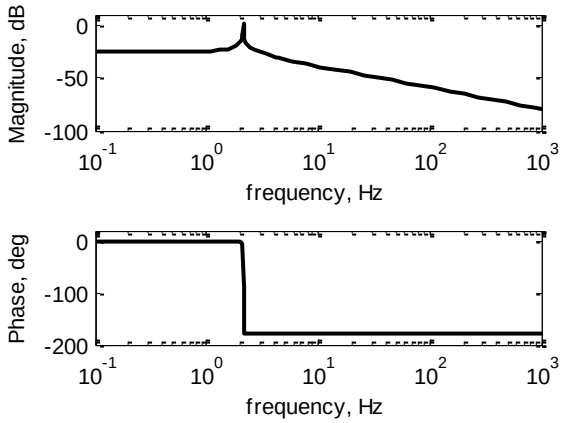

Figure B1. Balance Bode diagrams (ζ = 0.0145 s^{-1} and ω_0 = 13.44 rad s^{-1}).

The displacement sensor has been used to acquire the arm displacement $x_N(t)$ only due the vibrations (without any PPT shots). For (B.3) if the FT of the $x_N(t)$ is known, it is possible to calculate the FT of the noise *N(t)* as follows[29]:

$$FT[N(t)] = \frac{FT[x_N(t)]}{H(s)} \tag{B.5}$$

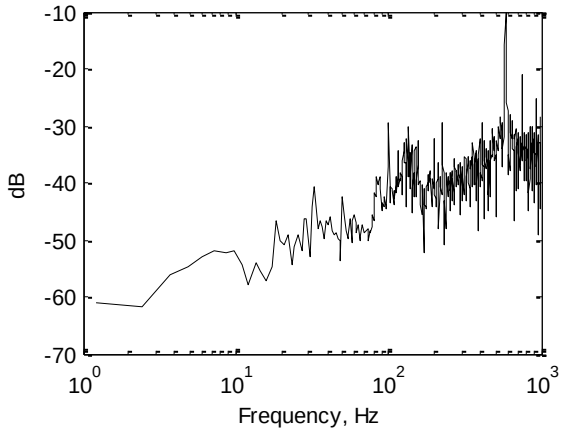

Figure B2. Induced noise *N(t)* FT.

The FT magnitude of the induced noise is shown in figure B2. Note that it reaches the maximum at about 600 Hz which is the rotational frequency of the pump.

Finally to quantify the order of magnitude of $x_N(t)$ and to compare this value with the ideal solution $x_{sol}(t)$, the root mean square (RMS) method has been used. The noise RMS has been evaluated[10] integrating the FT of $x_N(t)$, whereas the RMS amplitude of the ideal solution is simply calculated as the ratio between its amplitude and $\sqrt{2}$ because $x_{sol}(t)$ is a sine wave for (12). The results are shown in figure B3. It has been found that, as the natural frequency of the balance is about 2 Hz, the noise RSM is < 2% of the ideal RMS amplitude, depending of the actual *Ibit* for (8). This justifies the reliability and the goodness of the data fitting estimated in terms of R-square (see section 3.2.3).

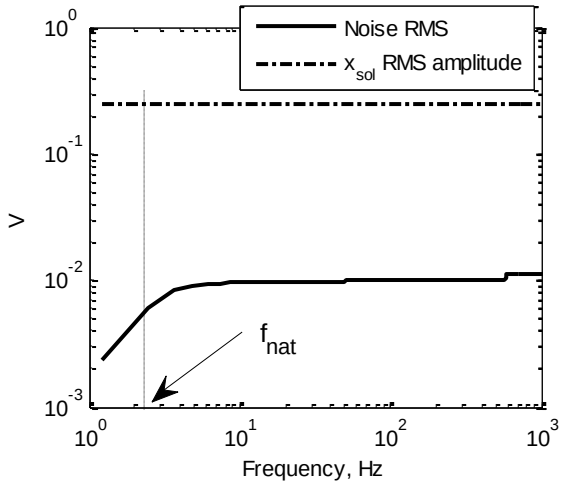

Figure B3. Comparison between the inducted noise RMS and the ideal RMS amplitude (in the example *Ibit* = 40 μNs)

References

[1]Jahn R G 1968 *Physics of electric propulsion* (McGraw-Hill, New York)

2Burton R L and Turchi P J 1998 Pulsed Plasma Thruster *J. Propulsion and Power* **14** 716-735.

[3]Schönherr T 2011 *Investigation of Performance and Plasma Dynamics of the Pulsed Plasma SIMP-LEX* (PhD thesis/The University of Tokyo)

[4]Mingo Perez A, Coletti M and Gabriel S 2012 A micro PPT for Nano-satellite applications: Design and experimental results *48th AIAA/ASME/SAE/ASEE Joint Propulsion Conference & Exhibit (Atlanta, USA)*

[5]Ciaralli S, Guarducci F, Coletti M and Gabriel S B 2013 PPTCUP: performances and extended test results *2nd IAAC Conference on University Satellites Missions and Cubesat Workshop (Rome, Italy)*

[6]Coletti M, Guarducci F and Gabriel S B 2011 A micro PPT for Cubesat application: Design and preliminary experimental results *Acta Astronautica* **69** 200-208

[7]Grubisic A N and Gabriel S B 2010 Development of an indirect counterbalanced pendulum optical-lever thrust balance for micro – to millinewton thrust measurement *Meas. Sci. and Technol.* **21** 105101

[8]Gamero-Castano M 2003 A torsional balance for the characterization of microNewton thrusters *Rev. Sci. Instr*. **74** 10

[9]Antropov N N *et al.* 2000 High Efficiency Ablative Pulsed Plasma Thruster Characteristics *3rd International Conference on Spacecraft Propulsion (Cannes, France)*

[10]Packan D, Bonnet J and Rocca S 2007 Thrust measurement with the ONERA micronewton balance *30th International Electric Propulsion Conference (Florence, Italy)*

[11]Koizumi H, Komurasaki K and Arakawa Y 2004 Development of thrust stand for low impulse measurement from microthrusters *Rev. Sci. Instr*. **75** 10

[12]Stephen R J *et al* 2001 Strain gauge based thrust measurement system for a stationary plasma thruster *Meas. Sci. and Technol.* **12** 1568-75

[13]Merkowitz *et al* 2002 A microNewton thrust-stand for LISA *Class. Quantum Gravity* **19** 1745-50

[14]Polzin K A *et al*. 2006 Thrust stand for electric propulsion performance evaluation *Rev. Sci. Instr*. **77** 105108

[15]Canuto E and Rolino A 2004 Nanobalance: an automated interferometric balance for micro-trhust measurement *ISA Trans.* **43** 169-87

[16]Riverhawk *Flextural pivot engineering data* http://www.flexpivots.com/

[17]Nawaz A *et al.* 2007 SIMP_LEX: systematic geometry variation using thrust balance measurements *30th International Electric Propulsion Conference (Florence, Italy)*

[18]PHILTEC Inc. 2010 *Product Data Sheet D63 Fiber-Optic Sensor*

[19]Krejci D, Seifert B and Scharlemann C 2011 Thrust Measurement of a Micro Pulses Plasma Thruster for Cubesats *1st IAAC Conference on University Satellites Missions and Cubesat Workshop (Rome, Italy)*

[20]Oppenheim A. V. *et al.* 1999 *Discrete-time signal processing* (Prentice Hall, 2nd edition)

[21]Taylor J R 1997 *An introduction to error analysis. The study of uncertainties in physical measurements* (University Science Books, 2nd edition)

[22]Iio J *et al* 2005 Evaluation on impulse bit characteristics of Pulsed Plasma Thruster by single impulse measurement *29th International Electric Propulsion Conference (Princeton, USA)*.

[23]Guarducci F, Paccani G and Lehnert J 2011 Quasi-steady MPD performance analysis *Acta Astronautica* **68** 904-914

[24]Tektronix Inc. *DPO3000 series digital phosphor oscilloscope user manual* http://www.tektronix.com

[25]Bell S *A beginner's guide to uncertainty of measurement* (Measurement Good Practice Guide No 11, issue 2.

[26]Kawahara K. *et al* 2003 Study on Plume Characteristics of Pulsed Plasma Thruster *28th International Electric Propulsion Conference (Toulouse, France)*.

[27]Guarducci F, Coletti M and Gabriel S 2011 Design and testing of a micro pulsed plasma thruster for cubesat application *32nd International Electric Propulsion Conference (Weisbaden, Germany)*

[28]Guman W J 1976 Solid Propellant Pulsed Plasma Propulsion System Design *J. Propulsion and Power* **13** 51-53.

[29]Rocca S 2011 ONERA micronewton thrust balance: analytical modelling and parametric analysis *Aerospace Science and Technology* **15** 148-154